Charles E. Andraka
e-mail: ceandra@sandia.gov

Julius Yellowhair

Kirill Trapeznikov

Jeff Carlson

Sandia National Laboratories,
P.O. 5800 Albuquerque,
NM 87185-1127, USA

Brian Myer
Department of Physics & Astronomy,
CAP 231, Appalachian State University,
525 Rivers St, Boone NC 28608, USA

Brad Stone

Kirby Hunt

Stirling Energy Systems,
4800 N Scottsdale Road,
Suite 5500 Scottsdale,
AZ 82521, USA

AIMFAST: An Alignment Tool Based on Fringe Reflection Methods Applied To Dish Concentrators

The proper alignment of facets on a dish engine concentrated solar power system is critical to the performance of the system. These systems are generally highly concentrating to produce high temperatures for maximum thermal efficiency so there is little tolerance for poor optical alignment. Improper alignment can lead to poor performance and shortened life through excessively high flux on the receiver surfaces, imbalanced power on multicylinder engines, and intercept losses at the aperture. Alignment approaches used in the past are time consuming field operations, typically taking 4–6 h per dish with 40–80 facets on the dish. Production systems of faceted dishes will need rapid, accurate alignment implemented in a fraction of an hour. In this paper, we present an extension to our Sandia Optical Fringe Analysis Slope Technique mirror characterization system that will automatically acquire data, implement an alignment strategy, and provide real-time mirror angle corrections to actuators or labor beneath the dish. The Alignment Implementation for Manufacturing using Fringe Analysis Slope Technique (AIMFAST) has been implemented and tested at the prototype level. In this paper we present the approach used in AIMFAST to rapidly characterize the dish system and provide near-real-time adjustment updates for each facet. The implemented approach can provide adjustment updates every 5 s, suitable for manual or automated adjustment of facets on a dish assembly line.
[DOI: 10.1115/1.4004357]

Keywords: CSP, dish stirling, alignment, fringe reflection, production

1 Introduction

Improper alignment of facets on a high-concentration dish system has been identified [1] as an important contributor to poor dish system performance. Because very few dishes have been assembled in large quantities, alignment approaches have been limited to field implementations with manual facet actuation. Diver et al. [2] describe a number of common approaches used in the past. McDonnell Douglas [3] implemented a Digital Image Radiometer alignment system consisting of a panel of computer-controlled light sources, with computer interpretation of the reflected images. These gave several points of data per facet, and automated the data collection and reduction process. However, data collection and reduction took several hours or more, and real-time adjustment was not accomplished. More recently, color look-back approaches [4,5] have been successful in a laboratory field environment with high quality mirror facets. However, these alignment approaches are time consuming field operations, typically taking 4–6 h per dish with 40–80 facets on the dish. Production systems will need rapid, accurate alignment implemented in a fraction of an hour.

Alignment tools have usually consisted of a target mounted near the engine location, with a "distant" observer or light source [4], or both a target and a camera/viewer at the 2-f location [5]. These approaches often require the dish to be placed in the horizontal (horizon) position, making access to the adjustments difficult and time consuming. In addition, the reflected light or image requires operator interpretation and a reasonably coherent image. Manufacturable facets may not have the image quality of laboratory dish systems explored in the past, making use of these alignment tools less effective.

The Sandia Optical Fringe Analysis Slope Technique (SOFAST) [6,7] was developed using fringe reflection techniques [8] to characterize facets and facet systems. Others [9,10] have also developed characterization systems based on fringe reflection techniques. Recent speed improvements in SOFAST for assembly line implementation have made it feasible to characterize the facet shape and rotations in real time, making use of this data feasible for alignment. The fringe method does not rely on coherent images, so a 2f approach with overlapping images on the target is feasible, leading to an alignment without extensive line-of-sight requirements, illustrated in Fig. 1.

The fringe reflection technique, also called Deflectometry in some literature, is a dynamic target method of determining the surface normals at many points across an entire surface simultaneously. A camera is positioned so as to see the reflection of an active target in the specular surface of interest, Fig. 2. A series of sinusoidal fringe patterns, or sinusoidally varying brightness patterns, are displayed on the monitor and the reflected images are recorded. Initially, a single cosine wave is displayed and then shifted 3 times by 90 deg each shift. This process provides four brightness levels for each pixel of the camera. The phase angle of the pixel can then be determined as

$$\tan[\phi(x,y)] = \left[\frac{I_4 - I_2}{I_1 - I_3}\right] \quad (1)$$

where I_n is the intensity measured at the camera pixel and n is the image sequence number. The phase angle is then simply the linear

Contributed by the Solar Energy Division of ASME for publication in the Journal of Solar Energy Engineering. Manuscript received January 17, 2011; final manuscript received May 31, 2011; published online July 28, 2011. Assoc. Editor: Eckhard Luepfert.

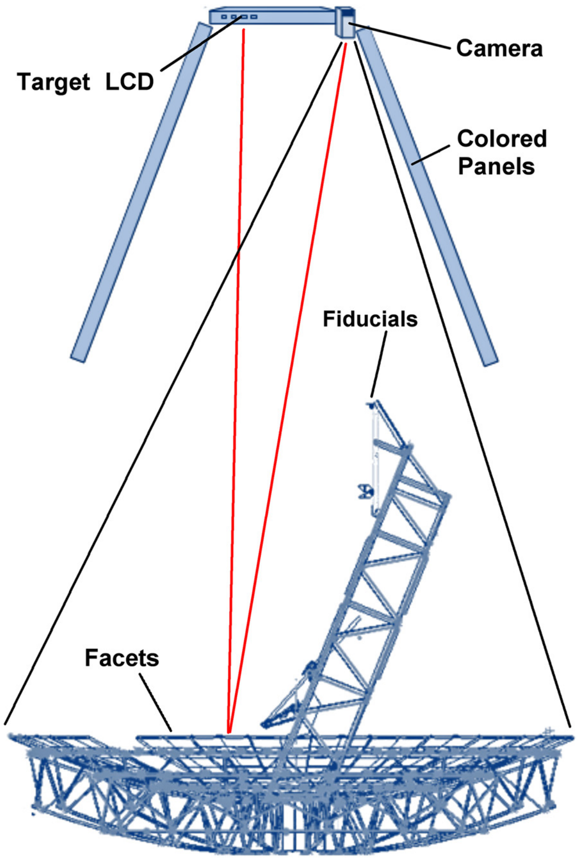

Fig. 1 AIMFAST physical layout with camera and target at the 2-f location. The solid black lines indicate the field of view of the camera, the dashed red lines indicate a typical reflected ray from the LCD screen to the camera.

position on the screen. This process is repeated for horizontal and vertical directions. The results may be refined by displaying finer fringe patterns, using the initial single pattern for an absolute screen position [6–8]. Given the camera lens position, the point at which each camera pixel ray intersects the specular surface, and the target point reflected to each camera pixel, a field of surface normal vectors is developed. This set of normal vectors is integrated to a surface shape description. The process is iterated if the surface shape does not match design. The measured surface normals (slope) can be fitted to any representative surface shape equations if desired.

In the Alignment Implementation for Manufacturing using Fringe Analysis Slope Technique (AIMFAST) system, an LCD display is used as a target, collocated with a camera near the 2f location of the dish system. In Fig. 1, the solid black lines indicate the camera field of view, and the red lines indicate a typical camera pixel, reflected off the facets to the LCD screen. The system may be set up vertically, horizontally, or any convenient orientation. The colored panels, not used in the current implementation, will help automatically locate facets that do not hit the target area. AIMFAST has been proposed to support production alignment of the Stirling Energy Systems (SES) SunCatcher™ dish-engine system. In addition, a mobile version is proposed to perform re-alignment or assessment of deployed dish systems. The mobile system consists of a camera and monitor mounted on a truck, supported with a laptop computer for data reduction. The concepts demonstrated with this portable system are directly applicable to the production facility implementation proposed. Further, digital communication can be implemented from AIMFAST to automated actuators to accurately implement the alignment adjustment commands.

This paper covers the initial implementation and testing of the AIMFAST system at Sandia National Laboratories, limited to data collection and analysis. Later planned papers will include actual re-alignment test results, an error analysis, and elevation-dependent measurements.

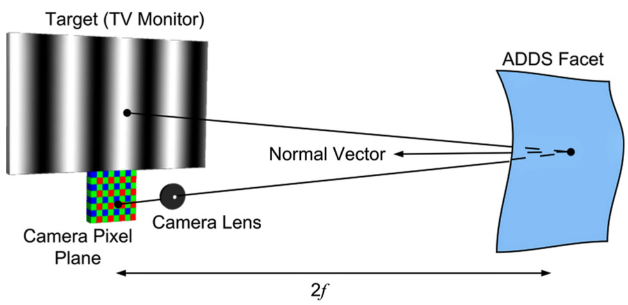

Fig. 2 Fringe reflection method physical layout

2 Approach

AIMFAST was implemented in a truck-mounted configuration for alignment of Stirling Energy Systems 25 kW_e dish system at Sandia National Laboratories in Albuquerque NM. In this paper, we collect "as-is" alignment data on the dish, and then perform a "virtual alignment," rotating the facets analytically in our optical model, in order to evaluate the data acquisition and reduction aspects of the AIMFAST software. Future work will include actually implementing the alignment adjustments to the dish facets.

The dish is an 11.4 m diameter parabolic collector consisting of 40 total gore-shaped facets arranged in two rows. Each facet can be adjusted in arbitrary radial and circumferential tilt to optimize the optical alignment of the dish, through the adjustment of the lengths of the outer two of three mounts. The fringe target consists of a 70" class (1.778 m diagonal, 16:9 aspect ratio) NEC brand monitor facing the dish near the 2-f position along the optical axis of the dish. The camera, a Basler 641fc, with a 6 mm lens, is mounted to the side of the monitor, and views the reflected image of the monitor in the dish. The optical axis of the camera is aligned to be perpendicular to the surface of the LCD monitor. The engine package is removed from the dish prior to data collection, in order to maximize the view of the dish from the 2f location.

The automated alignment process requires that the system first determine the location of the camera and target screen relative to the dish. We perform a photogrammetric technique on key natural design features located on the dish system to locate the camera and screen in the Dish Coordinate System (DCS). The DCS origin is at the vertex of the parabola, with the z axis along the optical axis of the dish. The x axis is to the right facing the collector and the y axis vertically upward. This extrinsic analysis approach has been tested for sensitivity of the camera position relative to the dish, and appears repeatable within 1 cm. The calculated camera position in dish coordinates can be refined based on physical measurements or fixtures to perfect the position estimated by photogrammetry. We used a laser distance meter, good to 2 mm, to determine the distance from the center of the LCD screen to the Outer Quad Split natural features on three inner facets, in order to correct the distance to the dish within 0.5 cm. The very small, typically less then 2–3 mm, correction applied through the use of the laser distance finder qualitatively validates the accuracy of the extrinsic analysis. A detailed sensitivity and error analysis will be the subject of a later paper.

Next, the camera pixels encompassing each facet are parsed out for individual consideration. This is important as each facet is individually positionable and, therefore, the dish surface is not continuous. These first two steps, the camera location and the facet pixel parsing, must be accomplished prior to alignment. A white, then black image are displayed on the monitor and the reflected image recorded, differenced, and thresholded. This provides a map of "active" reflective pixels, or camera pixels that can "see" the monitor in the facets. If facets are not sufficiently prealigned so that the camera can see the monitor reflection in each facet, they can be set with physical measurements, through a search algorithm (facets sequentially moved until the monitor reflection is detected) or through colored runout areas next to the monitor, as seen in Fig. 1.

The heart of the system is the fringe analysis routine. Sinusoidal fringe patterns are displayed on a large LCD monitor colocated with the near the 2-f location, and the surface normals can be determined with standard fringe reflection methods similar to SOFAST [6,7]. The rotational position of the facet is determined and compared to the design facet rotation. The pointing angle of the facet can be represented in one of several ways [11], including a single representative normal vector of a fitted shape, an average of surface normal error, or a weighted average error. The facets' calculated pointing angle errors are used to calculate corrections to facet rotations or mount adjustments, and passed to the worker or an automated tool. The collection of fringe image data and reduction to facet rotation requirements takes 4–5 s.

The process is iterated several times until the facet rotational errors are within specification. In Ref. [1], we found that, for this particular dish design, the specification should be 0.25 mrad RMS random alignment error. Because AIMFAST measures about 20,000 points per facet, we believe that alignment measurements significantly lower than this specification can be repeatedly made, but this needs to be verified in a complete error analysis in a later paper. After tightening or otherwise fixing the adjustment mechanism, a final image is acquired and the flux profile on the receiver surface is modeled and archived. A side product of the process is a characterization (focal lengths, twist, and slope error) of each facet in place on the dish.

The AIMFAST system is in prototype testing at Sandia National Laboratories. Initial results are promising. In this paper, the facets are not physically moved, but the calculated rotations are applied analytically and then the optical model is run to verify resultant flux pattern predictions, in order to validate the data reduction steps.

3 Results

A set of data was collected from an early prototype SES SunCatcher™ dish system at Sandia. The dish was previously aligned with the color lookback method and was known to have a boresight error due to a layout error on the printed color target. In addition, attempts had been made to perform "hot alignment" adjustments, or changes to the alignment though observation of the reflected on-sun image. The previous color lookback alignment was performed at 0-deg elevation to provide for distant viewing, and the target accounted for structural deviations from the 0-deg alignment elevation to the 40-deg nominal tracking elevation. The dish had been fluxmapped to characterize the flux pattern as currently aligned. The AIMFAST data was collected in the "service" position, or 20 deg below horizon, providing ready access to mount the monitor at the 2f location. The engine was removed to allow full view of the dish from the 2f location. The alignment was compared to the design alignment of the SES dish system, which is designed to evenly distribute the collected energy over the active portions of the heater head. The dish requires specialized alignment adjustment tools which were not available at the time of this test due to bug fixes at the manufacturer of the tools. Therefore, the current alignment was characterized, and a "virtual alignment" performed to evaluate the efficacy of the AIMFAST approach.

The key design points on the dish were selected as the "Outer Quad Splits" (OQS) on each facet. Each facet has eight lites of

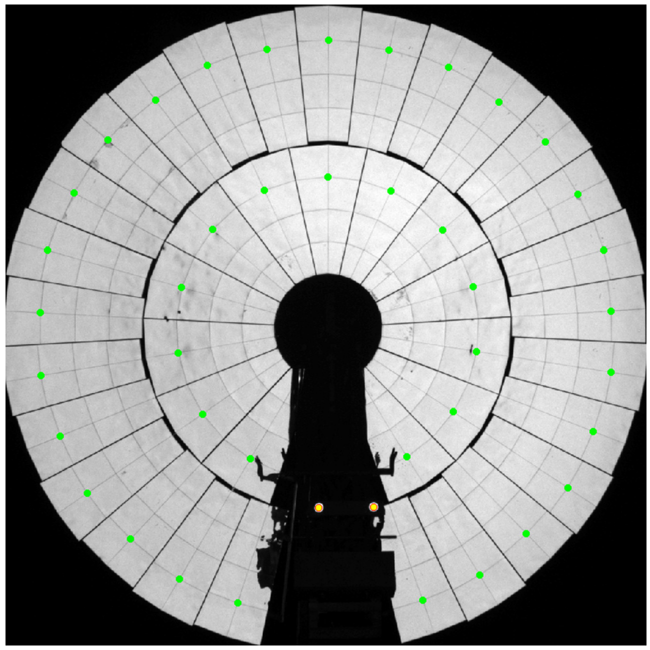

Fig. 3 Mask image of dish showing key physical locations including OQS and two fiducials at the engine mount location

glass. The OQS is the location at which the four outermost lites share a common corner. This is a more reproducible point than mirror edges, due to potential tolerancing of the facet lites. This provides 40 key locations on the "plane" of the mirrors (Fig. 3). An additional two points were located at the mounting bolt holes for the engine package, providing points well out of plane with the mirrors. These points were located with magnetically mounted reflective fiducials, and the center of the fiducials found with a centroid calculation. The engine fiducial locations were weighted by a factor of 20 over the mirror points, so that the alignment would be along the axis defined by the origin of the DCS and the engine location rather than an axis perpendicular to the mirror "plane." Empirical tests indicate that an equal number of points out of plane (2×20) to those on the mirrors (40) is sufficient weighting to define the boom axis. The amount of this additional weighting of the engine fiducials is currently under further evaluation for optimization. The 40 points on the dish (one for each facet) and the fiducials define the DCS, as there is no physical reference point for the origin of the DCS. Given the design location in 3 dimensions of these key points and the pixel locations in 2 dimensions on the camera pixel plane, an extrinsic (photogrammetric) analysis is performed that locates the camera in the DCS.

The mirror rotation errors were determined by a simple averaging of the normal vector errors over the entire facet. Other approaches could be used and are explored in Ref. [11]. The measured normal vector at each pixel location was compared to the design facet at the same location. This operation was performed in each facet coordinate system (FCS), rather than the DCS. The facet shape, locations, and rotations (tilts) are defined in a CIRCE2 optical model input deck, directly read by AIMFAST. The alignment strategy contained in the CIRCE2 input deck rotation of each FCS is relative to the DCS. The 40 facets do not have the same aimpoint, in order to fill the pedestal gap shadow. Therefore, by placing the measured data into each design facet coordinate system, the orientation of the measured surface normal at each point on the facet can be compared to a simple parabola of rotation (design facet shape) and a pointing error of each normal vector across the facet developed. The average pointing error across a facet should then be driven to zero by physically (or in this test case, analytically) rotating the facet in the direction opposite of the error. Figure 4 shows the resulting facet pointing

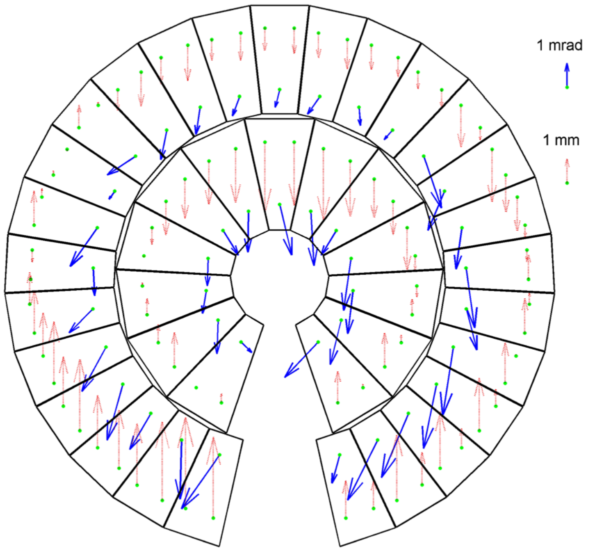

Fig. 4 Mirror tilt errors as determined by AIMFAST. The solid blue vectors represent the magnitude and direction of the mirror tilt away from the alignment strategy, anchored to the inner mirror mount. The red vectors indicate the magnitude of the outer mirror mount adjustments needed to resolve the error. An upward adjustment indicates a longer stud is needed, downward is shorter.

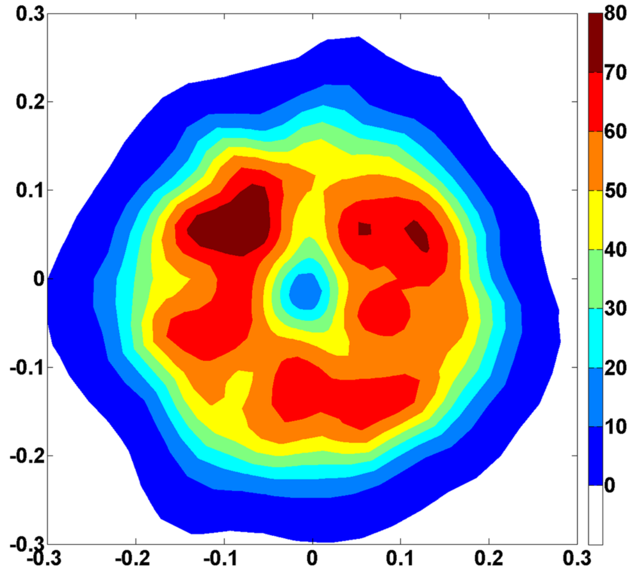

Fig. 5 CIRCE2 prediction of flux on a flat plate near the receiver tube location, based on AIMFAST measured facet position and shape. The flat target is at 6.91 m from the dish vertex.

errors, represented by solid blue vectors showing direction and magnitude of the errors. The general trend of a downward-pointing error vector is indicative of the known boresight error on this dish. The figure also shows the mounting stud length corrections needed to remove the alignment errors, as red vectors. Only the outer two (of three) mounts are adjusted, the mirror rotates about the inner mount location. The mount length correction magnitudes are shown as a vertical vector, with "up" meaning lengthen the mount.

The alignment strategy was developed with multiple runs of CIRCE2 [12] models on design facets. The strategy fills in the "shadow" of the pedestal notch of the dish, while minimizing the impact on the aperture size required for full intercept of reflected energy. In addition, structural deflections and rotations are accounted for, such that the alignment strategy at the alignment position (vertical on an assembly line, below horizontal in the field) is deviated from design by the same amount as structural deviations. In addition, the weight of the engine, removed during alignment, is factored into the gravity deviations. Total gravity-induced structural deviations resulted in facet rotations up to about 1 mrad. Thus, at a prescribed "golden angle" elevation, 40 deg in this case, the alignment should be at the design condition. The "golden angle" can be determined by an energy-weighted or revenue-weighted average dish elevation, and may also take into account the relative severity of combined deflections at different elevation angles, so as to minimize impacts to the life of the engine through increased flux pattern errors. This alignment strategy is contained in the CIRCE2 input deck, which is directly read by AIMFAST, and augmented with a spreadsheet file of modeled structural deflections. The development and application of structural deviations will be covered in detail in a future paper.

The field of as-measured facet normal vectors, in each FCS, was placed into the CIRCE2 optical model, replacing the design analytical facet, and the flux profile from the dish was predicted on both a flat target and on the engine receiver cavity. It was important for this model to separate the facets into individual facet definition files, rather than modeling the entire dish set of normal vectors, in order to perform the virtual alignment. Figure 5 shows the CIRCE2 prediction of flux from the dish in its current condition, onto a flat target simulating the fluxmapper water-cooled target. The measured facet positions are corrected for structural deflections from −20 deg data collection elevation to 40 deg on-sun elevation, for comparison to the fluxmapper on-sun data. The AIMFAST system is unable to measure to the edge of facets near the pedestal gap, as the engine support boom blocks the camera view partially. Therefore, the CIRCE simulation under-predicts flux in the 12-o'clock portion of the target board. Figure 6 shows the measured flux profile using the fluxmapper system with the dish at approximately 40-deg elevation, and shows good qualitative agreement to the CIRCE2 prediction, except in the shaded 12:00 region due to the lack of AIMFAST data in this area. Both the fluxmapper target and the CIRCE2 analytical target were placed at 6.91 m from the dish vertex, or 0.203 m behind the design focal plane of the dish. The flux level is not 0 at the edge of the fluxmapper target, which causes a slight error in the total

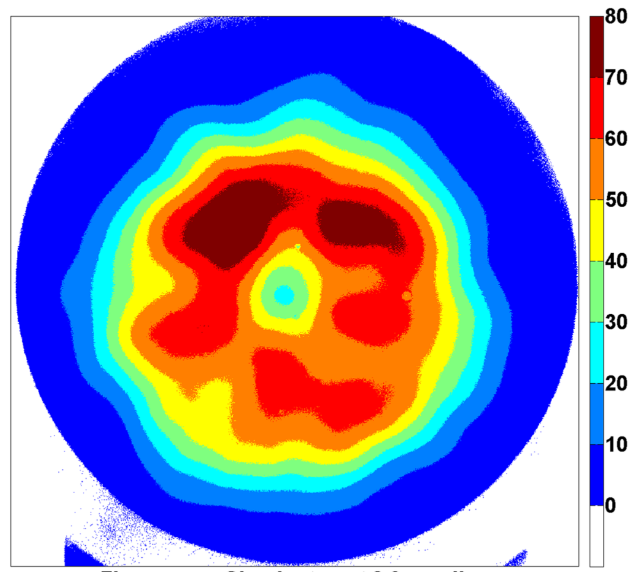

Fig. 6 Fluxmap of the dish on a flat target at 6.91 m forms the dish vertex, in the pre-alignment condition

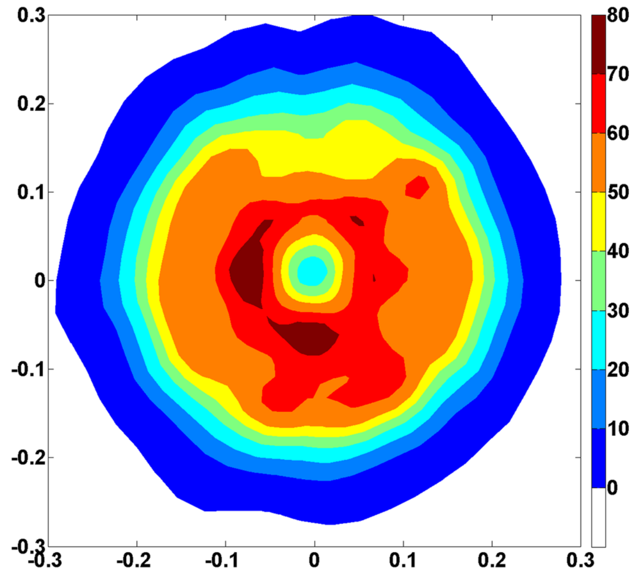

Fig. 7 CIRCE2 prediction of flux profile after mirror facets are analytically rotated the AIMFAST-prescribed amount

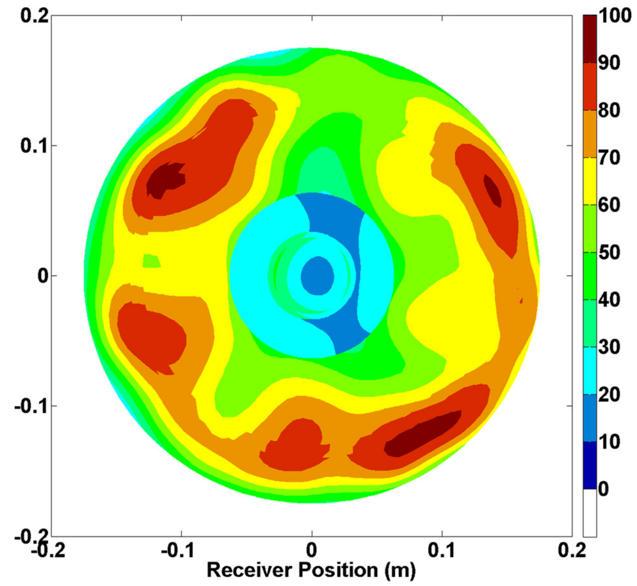

Fig. 8 CIRCE2-predicted flux profile on receiver tubes based on AIMFAST measurement of facet normals and deviations

integrated flux pattern, and thus a slight over-estimation of the local flux levels. The fluxmapper target is 0.61 m diameter. The general agreement between Figs. 5 and 6 provides confidence that our measurements and CIRCE2 model realistically reflect the physical condition of the dish.

We then performed the "virtual alignment" of the dish. In this step, we rotated (tilted) the facet normal vector data about the inner stud location by the amount prescribed in Fig. 4. This simulates the process of applying the alignment to the dish. In a real system, in order to accommodate hysteresis in the tools and other uncertainties, we would repeat the process until the alignment was accurate. Each loop through the process would take 4–5 s for data collection and reduction, and a few seconds for automated adjustment or a few minutes for manual adjustment. We then ran CIRCE2 on this modified data. Figure 7 shows the virtually aligned flux profile on a fluxmapper target, and demonstrates that, even without iteration, a marked improvement in flux uniformity can be accomplished. The peak local flux drops nearly 20%, and the distribution around the entire heater head area is remarkably smooth. Again, the boom blockage of the AIMFAST system causes a slight under-prediction at the 12-o'clock position. The remaining slight peaks in the profile are caused by slightly long facet focal lengths.

We ran CIRCE2 again with the as-measured data and the virtually aligned data, replacing the flat target with the receiver cavity, and evaluated the flux profile on the heater head tubes and the center ceramic cone. Figure 8 shows the predicted profile as measured, while Fig. 9 shows the improved profile after virtual alignment. The revised alignment clearly shows improvement in distribution of flux and a reduction in the peak fluxes. The remaining highest peak fluxes are due to a long focal length on some facets, which has been resolved in later systems through application of SOFAST characterization on the facet production floor, leading to production process improvements.

4 Next Steps

The most obvious next step is to perform a physical alignment on a dish, and then repeat the fluxmap process to qualify the alignment. These results will be reported in Ref. [13]. The complete alignment system will then be ruggedized and applied to the near-field assembly line for the SunCatcher™ systems. In addition, a truck-mounted system will be developed for implementing field repairs, facet replacements, and alignment checking.

While the prototype development focuses on an immediate need for dish systems, we expect this approach can be used for production alignment of trough and tower concentrated solar power (CSP) systems, with adaptation. The fundamental building blocks of photogrammetric camera positioning, parsing of facet data, fringe characterization of the facets, and rapid and efficient data reduction remain the same in each case. The screen size would need to be expanded, through monitor walls, projection systems, and moveable systems, to accommodate the facets used in those CSP systems, which are flat in one (trough) or two (heliostats) dimensions.

A complete error analysis and qualification of the system must be performed and reported in a later paper. The methods of accounting for gravity-induced deflections as well as extrinsic positioning of the camera must be refined and documented.

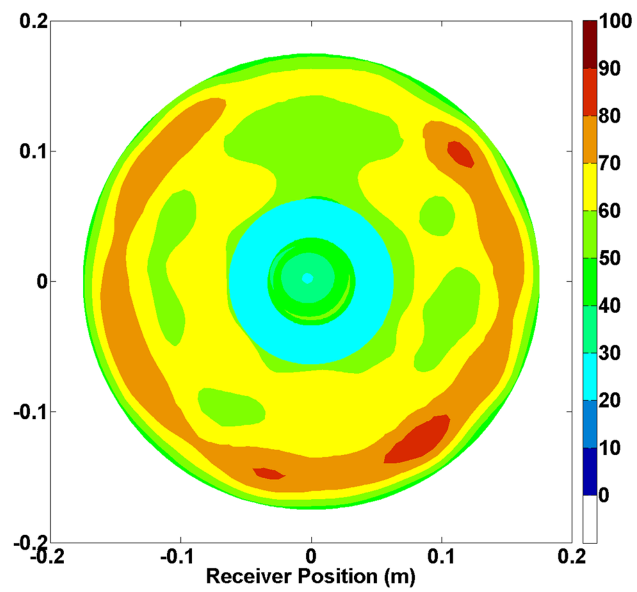

Fig. 9 CIRCE2-predicted flux profile on receiver tubes after virtual re-alignment of the measured normals

5 Conclusions

A method for rapid evaluation and alignment of dish systems, AIMFAST, has been demonstrated. The close correlation of the measured data as projected by CIRCE2 and the fluxmap measurements on the dish give high confidence that the process can be used for accurate alignment. Since the fringe reflection method does not require coherent images, the alignment tool is robust even with commercial-quality facets. A virtual alignment was performed, and demonstrates the potential of the alignment approach. The data acquisition and reduction speed falls well within goals needed to reach high rate production. A 4–5 s cycle time is sufficient for near-real-time tool adjustment through electrical actuation or manual adjustment with data displays at the adjustment location. While the AIMFAST system meets the speed goals for production, it also eliminates subjective image evaluation and accommodates facets across the range of manufacturing specification. The approach appears to provide a tool suitable for alignment of dish systems in a production environment, with improved speed and accuracy over existing methods.

The next steps include demonstration of alignment implementation in hardware, both in a prototype assembly line process as well as a portable re-alignment system for field repairs. We expect this system will be useful for production alignment of other CSP systems as well as dishes.

Acknowledgment

This manuscript has been authored by Sandia Corporation under Contract No. DE-AC04-94AL85000 with the U.S. Department of Energy. The United States Government retains and the publisher, by accepting the article for publication, acknowledges that the United States Government retains a non-exclusive, paid-up, irrevocable, world-wide license to publish or reproduce the published form of this manuscript, or allow others to do so, for United States Government purposes.

References

[1] Andraka, C. E., Yellowhair, J., and Iverson, B. D., 2009, "A Parametric Study of the Impact of Various Error Contributions on the Flux Distribution of a Solar Dish Concentrator," Proceedings of the ASME (2010) 4th International Conference on Energy Sustainability, ASME, Phoenix AZ USA May 17–22, ES2010-90242.

[2] Diver, R. B., 1992, "Mirror Alignment Techniques for Point-Focus Solar Concentrators," Sandia National Laboratories, Albuquerque, NM, USA, SAND92-0668.

[3] Blackmon, J. B., and Stone, K. W., 1993, "Application of the Digital Image Radiometer to Optical Measurement and Alignment of Space and Terrestrial Solar Power Systems," 28th Intersociety Energy Conversion Engineering Conference Proceedings, American Chemical Society, Washington DC, **2**, pp. 2.563–2.570, 93217.

[4] Andraka, C. E., Diver, R. B., and Rawlinson, K. S., 2003, "Improved Alignment Technique for Dish Concentrators," Proceedings of ISEC 2003: 2003 International Solar Energy Conference, ASME, Kohala Coast, Hawaii Island, Hawaii USA, SAND2003-0258C.

[5] Steffen, B. J., Andraka, C. E., and Diver, R. B., 2003, "Development and Characterization of a New 2-f Alignment Method for the Advanced Dish Development System," Proceedings of ISEC 2003: 2003 International Solar Energy Conference, ASME, Kohala Coast, Hawaii Island, Hawaii USA.

[6] Andraka, C. E., Sadlon, S., Myer, B., Trapeznikov, K., and Liebner, C., 2009, "Rapid Reflective Facet Characterization Using Fringe Reflection Techniques," Proceedings of Energy Sustainability (2009), ASME, San Francisco, CA USA, July 19–23, ES2009-90163.

[7] Andraka, C. E., Sadlon, S., Myer, B, Trapeznikov, K., and Liebner, C., 2009, "SOFAST: Sandia Optical Fringe Analysis Slope Tool for Mirror Characterization," Proceedings of Solar Paces 2009, Solar Paces, Berlin, Germany, Sept. 15–18.

[8] Bothe, T., Li, W., von Kopylow, C., and Jüptner, W., 2004, "High Resolution 3D Shape Measurement on Specular Surfaces by Fringe Reflection," Optical Metrology in Production Engineering, Proceedings of SPIE, W. Osten and M. Takeda, eds., Bellingham, WA. USA, Vol. 5457, pp. 411–422.

[9] Ulmer, S., Marz, T., Prahl, C., Reinalter, W., and Belhomme, B., 2009, "Automated High Resolution Measurement of Heliostat Slope Errors," Proceedings of Solar Paces 2009, Solar Paces, Berlin, Germany, Sept. 15–18.

[10] Heimsath, A., Platzer, W., Bothe, T., and Wansong, L., 2008, "Characterization of Optical Components for Linear Fresnel Collectors by Fringe Reflection Method," Proceedings of Solar Paces 2008, Solar Paces, Las Vegas, NV USA, Mar. 4–7.

[11] Yellowhair, J., Andraka, C. E., Trapeznikov, K., and Hunt, K., 2010, "Alignment Strategy Development for Imperfect Facets on a Dish Concentrating System," Proceedings of Solar Paces 2010, Solar Paces, Perpignan, France, Sept. 21–24.

[12] Romero, V. J., 1991, "CIRCE2/DEKGEN2: A Software Package for Facilitated Optical Analysis of 3-D Distributed Solar Energy Concentrators – Theory and User Manual," Sandia National Laboratories, Albuquerque, NM, SAND91-2238.

[13] Andraka, C. E., Yellowhair, J., Finch, N., Carlson, J., Francis, M., Hunt, K., Raffa, C., and Kulaga, T., 2011, "AIMFAST: Initial Dish System Alignments Results Using Fringe Reflection Methods," Proceedings of ASME 2011 5th International Conference on Energy Sustainability and 9th Fuel Cell Science, Engineering and Technology Conference, ASME, Washington DC USA, Aug. 7–10, ESFuelCell2011-54453.